Received: 11 September 2023 | Revised: 19 October 2023 | Accepted: 26 October 2023 | Published online: 27 October 2023

RESEARCH ARTICLE

Archives of Advanced Engineering Science
2023, Vol. 00(00) 1–13
DOI: 10.47852/bonviewAAES32021716

BON VIEW PUBLISHING

Excellent Miniature Thin Film Dielectric Elastomer Sensors for Robot Fingers Used in Human-Robot Interaction

Seiki Chiba[1],* and Mikio Waki[2]

[1]*Chiba Science Institute, Japan*

[2]*Wits Inc., Japan*

Abstract: Traditional sensors used to measure properties such as deformation and pressure often use materials such as metals, ceramics, piezos, and polymers. However, since many of these materials are hard, it can be difficult to measure them with a single sensor when the pressure or elongation applied to the object changes. In this experiment, a dielectric elastomer thin-film pressure sensor (0.2 mm) was fabricated using hydrogenated nitrile rubber with significantly improved hardness and elongation. This single sensor can accurately measure pressure from 1 gf to 20 kgf. Also, the response speed was 50 ms, which was sufficiently fast. A dielectric elastomer stretch sensor was also developed. This sensor uses elastic and flexible single-walled carbon nanotubes as dielectric elastomer electrodes for the hydrogenated nitrile rubber. This greatly improved the mechanical flexibility and stretchability of the stretch sensor, making it possible to operate it as a sensor even at 400% elongation. By attaching this stretch sensor to the robot's finger closely, it is possible to detect the dynamic movement of the robot's finger and to detect the force (pressure) when the fingertip touches the target object with the above pressure sensor. In addition, by using the small diaphragm-type dielectric elastomer actuator, it was confirmed that the sensation of the robot's touching an object could be fed back to the human finger. As a result, it is thought that the feeling of the robot's finger touching an object could be driven more realistically and accurately. In addition, both a dielectric elastomer stretch sensor and a dielectric elastomer pressure sensor were attached to the finger of the robot, and the movement of the human's finger was sensed and the force (pressure) when the finger touched the object was also able to be detected.

Keywords: dielectric elastomer, sensor, actuator, stretch, pressure, large deformation, carbon nanotube spray

1. Introduction

Some composite materials that can be utilized as sensor materials are piezoelectric composite materials [1], conductive polymer materials [2], bimetals [3], and others. The first two are materials that combine the advantages of both organic and inorganic materials in a matrix. The others are used in temperature sensors and other devices by combining dissimilar metals. In addition, for engineering sensors, using materials such as new metal materials (e.g., liquid metal), high-performance polymer materials, fine ceramics, composite materials based on additive manufacturing, and others combined with electronics and biotechnology, may be able to meet various needs in the 21st century. They are expected to be used in cutting-edge technologies that support a variety of industries and economies [4, 5]. Examples include robotics, wearable electronics [6], epidermal electronic systems [7], human-machine interfaces [8], soft robotics [9], other biomedical devices [10, 11], and related systems [12]. In most of these systems, sensory feedback plays an important role in considering efficiency and performance accuracy. Tactile sensors currently in use include pressure [13], strain [14], shear [15], force [16, 17], and vibration sensors [18]. Through contact between objects and their sensors, human contact perception can be emulated in robots and other machines. Common transduction principles used in this type of sensor include piezoresistive, piezocapacitive, piezoelectric, triboelectric, and electrical resistance [19]. However, those materials are not soft enough, and their mechanical flexibility and stretchability need to be improved in order to realize sensors that adequately follow changes in elastomers and electrodes caused by changes in pressure or arm/finger movements. As an example, multi-walled carbon nanotubes(MWCNTs) were dispersed on a silicone elastomer to create strain sensors based on the change in resistance [20]. However, after dispersion, the sensor was annealed to increase its strength. As a result, the sensor became stiff and its elongation was limited. As the example of a liquid-type sensor, wearable sensors including skin sensors based on glycerol and graphene quantum dots (Gly-GQDs) as sensing units were proposed [21]. In addition, a fluidic strain sensor based on a biocompatible conductive poly (3, 4ethylenedioxythiophene) polystyrene sulfonate multiwall carbon nanotube (PEDOT:PSS/MWCNT) liquid was also proposed [22]. The elongation of these sensors was 150 mm. As a sensor using light, a novel flexible mechano-optical sensor by modulating the transmittance of ecoflex/

*Corresponding author: Seiki Chiba, Chiba Science Institute, Japan, Email: chiba.jetpilot.seiki@gmail.com

molybdenum disulfide (MoS2) was also proposed [23]. However, the elongation of this sensor was also a maximum elongation of 150.

One of the goals of the experiments was to increase the finger's pressure sensitivity more sensitive and capable of measuring even smaller values using an extremely thin and small sheet-type dielectric elastomer (DE) pressure sensor. Hydrogenated nitrile rubber (HNBR) was used as the dielectric material. The previously synthesized HNBR ver.3 was too hard, so the pressure that could be measured was 4 to 120 kgf [24]. To measure smaller pressure therefore, an attempt has been made to improve the elongation (hardness) significantly by adjusting the amount of cross-linking agent added and breaking some of the double bonds in this experiment. Table 1 shows a comparison of the current pressure measurement target values and the previous result.

Table 1
Current pressure sensor goals and previous results

Material	Size and thickness of test sample	Measurement range
HNBR ver.3	20 mm diameter × 0.2 mm	4 kgf to 120 kgf
HNBR ver.6	Same as above	1 gf to 20 kgf

Note: HNBR ver.3 is the material used last time, and HNBR ver.6 is the material used this time.

Additionally, the development of a DE stretch sensor (DESS) with greater stretchability and flexibility using single-walled carbon nanotube (SWCNT) electrodes and this HNBR was attempted, in order to significantly improve the mechanical flexibility and stretchability of the DE sensors. Furthermore, using this stretch sensor, an experiment to sense the movement of the robot's finger and detect the force (pressure) when the fingertip touched the target object with the DE pressure sensor (DEPS) was tried. An experiment using a small diaphragm-type transducer DE actuator to confirm that the sensation of a robot finger touching an object can be fed back to a human finger was also conducted.

2. Background of Dielectric Elastomer Sensors

DE was developed starting in 1991 by Chiba et al. [24] at the Stanford Research Institute (SRI International, USA). The DE can be an actuator, a sensor, and a generator with the same structure.

The structure of the DE is simple, consisting of an actuator sandwiched between flexible electrodes above and an elastomer (polymer) below. When a voltage is applied to the electrodes, the upper and lower electrodes are attracted by the Coulomb force and the elastomer is crushed, resulting in lateral elongation of the elastomer. The structure and principle of a DE sensor (DES) (see Figure 1) is the same as a DE actuator (DEA), and the drive principle is inversely proportional to DEA output and elongation [25–27].

The relationship between DES and capacitance can be expressed by the following simple equation:

$$C = \varepsilon \varepsilon o S/d \tag{1}$$

where C is the capacitance (F), $\mathcal{E}$ and $\mathcal{E}o$ are the permittivity of free space and the relative permittivity (dielectric contact) of the polymer, respectively (F/m), S is the electrode area (m^2), and d is the distance between the electrodes (m).

Figure 1
Structure and principle of DES

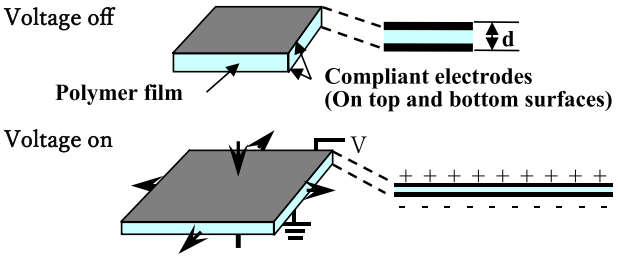

Also, the changed area can be obtained from the following formula:

$$S = Cd/\varepsilon\varepsilon\, o \tag{2}$$

For the elongation, l is as follows:

$$l = Cd/w\,\varepsilon\,\varepsilon\; o \tag{3}$$

where l is the length of the DES and w is its width.

Electrode materials, electrode attachment methods, elastomer improvements, electrical circuits, and other related technologies are being developed as DE/DES components. In order to produce flexible electrodes, the materials used for them include metal foil (including liquid metal), carbon grease, carbon particles (e.g., carbon black), carbon nanotubes (CNT), and conductive polymers [5, 24, 28]. If a larger electrode deformation is required, it is better to use highly conductive CNTs (especially single-wall CNTs) (Chiba et al., 2020). Liquid metal or carbon grease is less suitable due to grease leakage. However, with good insulation, leaks are less likely to occur, but this imposes some restrictions on operation [5]. A PS composed of CNT-polydimethylsiloxane (CNT-PDMS) composite electrodes and a porous polymer dielectric layer was proposed as a medical wearable sensor [29]. While the concept is interesting, this wearable sensor might not work well because the electrodes are not flexible enough and the polymers used are stiff. Carbon black and several different polydimethylsiloxanes (PDMS) have been studied on electrode compositions also [30]. Electrodes can be made by dissolving CNT or carbon black in a solvent, mixing in a small amount of binder, and applying it to the elastomer with a brush or paint [24, 31]. The CNT ink using a finger or a slightly larger brush, which left traces of the brush or finger on the surface of the electrode, was applied. Unfortunately, this resulted in an uneven thickness of the electrode [31].

Five layers of DES were used to detect the position of a robot fish fin [32]. A softer material was prepared by adjusting the dangling chains of the elastomer and the cross-linking agent was prepared. A sheet-type DEPS was created, demonstrating usefulness of the sensor [24]. However, small pressures could not be measured [24]. The usefulness of the DES made of thin layers of soft dielectric materials (acrylic, silicon, etc.) also have been discussed [27]. A softer commercial acrylonitrile-butadiene rubber (NBR) containing a large amount of plasticizer as the base material for the dielectric layer of the DE was used [33].

As an example of circuit research, K. Jung et al. used a system that mixes a low-frequency signal for operation with a high-frequency signal of a small amplitude for detection to realize DEA drive and motion detection using modulation techniques [34]. Böse and Fuß [35] conducted an experiment using a thicker

mat-type pressure sensor instead of a sheet-type DE. They also considered making the DES structure a waveform and making it into an array. Unfortunately, however, the size of the sensor is larger than that of the sheet type, and the material is silicon, so it might not be able to expand much, which might limit its application [36]. Side-by-side silicone-based diaphragm-type DEs to enable cooperative sensing and tactile functions were proposed [37]. Regrettably, silicone has low elongation, and the diaphragm-type DE array type is a fixed-point measurement type sensor similar to a sensor that measures resistance. It could therefore be difficult to accurately follow the movement of limbs and measure them [24].

Finally, as an example of a possible application, Walker & Anderson [38] carried out a study in which a DESS was attached to a diver's wetsuit and movement was monitored. As another example of system research, it was pointed out that the DEA/DES system, which combines a DES and a DEA, could assist in the movement of patients' fingers, hands, feet, etc., and could possibly be used to accurately evaluate the progress of physical rehabilitation [24]. Venkatraman et al. [39] attempted to measure blood pressure using a DE cuff device.

It is highly possible that the DE could be used simultaneously as an actuator and pressure and/or position sensor [24]. In the very near future, it might also become possible to create intelligent robot limbs and nursing care equipment using DESs, which would assist the movement of a patient's fingers, hands, feet, and so on. Furthermore, this technology could possibly evaluate the rehabilitation status with great accuracy [24]. However, developing such devices will require further improvements in DEA/DES performance. The main factors for this are the improvement of the conductivity of the electrode and its flexibility, and the flexibility of the elastomer should also be sufficiently improved [24].

3. Research Methodology

The purpose of this experiment is the following two points.

(1) A DESS and a DEPS, which are made by combining SWCNT electrodes with greater stretchability and flexibility and a film with improved hardness and elongation of HNBR, are attached to robot's finger, and the motion of the finger is sensed, and the force (pressure) when the finger touches the object is detected.

(2) In addition, assuming the use of a virtual system or the like, in order to drive the robot's finger as the human operator wishes, stretch sensors are attached to the fingers of the human and the robot, and a system is constructed to transmit the movement of the fingers from the human to the robot. Thus, a system by replacing human finger movements with robot fingers can be demonstrated. An additional experiment was conducted in which a vibrator using a small DEA was attached to the fingertip of the robot, and the sensation of contact with the object was transmitted to the human finger.

3.1. Adjustment of elongation (hardness) and film formation of hydrogenated nitrile rubber (HNBR)

HNBR (prepared by ZEON Corporation) is a material that is laid under the car engine to absorb the vibration of the engine. HNBR can be used in relatively hot environments and has excellent heat resistance, oil resistance, dielectric strength, and a high dielectric constant [24]. Therefore, in the near future, HNBR is expected to be utilized in a high-power DEAs or wave power generation. However, it is now used to absorb engine vibrations, so it is stiff and not suitable for DEs. An attempt has been made to improve the elongation (hardness) by adjusting the amount of the cross-linking agent added and cutting some of the double bonds. The following shows how to adjust the amount of cross-linking added and how to cut a part of the double bond:

(1) How to adjust cross-linking agents:

HNBRs were dissolved in MEK (methyl ethyl ketone), organic peroxide (1,3 1,4-bis (t-butylperoxyisopropyl benzene)) was added, and it was mixed with a dispersion machine. Next, it was dried naturally to remove the solvent and obtain a mixture. Finally, the mixture was pressed at 150 ° C and made into a film.

(2) Dangling bond reduction method:

By reducing the double bond of the HNBR, the generation of dangling bonds caused by oxidative deterioration or other processes, originating from the double bond, was reduced. In other words, by improving the hydrogenation rate (crushing the double bond with hydrogen), both the generation of double bonds and the organic peroxide as the starting point were eliminated as much as possible, which in turn greatly limited the double bonds. After carefully hand-casting the HNBR film, 4 locations on the film were selected and the film thickness was checked to make sure that the film thickness was uniformly 200 μm, using a digital thickness gauge (SMD-565A-565A-565A) by TE-CLOCK Co., Ltd.

3.2. Tensile test

A tensile test of the dumbbell-shaped test piece was performed using the Orientech tabletop material tester STA-1150. The displacement velocity was set to 500 mm/min.

3.3. Electrode materials for DES and their adhesion method

SWCNT (Zeon corp. ZEONANO®-SG10) was selected as a highly conductive material that can be molded into a compliant electrode. A sprayable CNT solution was developed to facilitate electrode fabrication. It was prepared by mixing dispersed CNTs and a binder. For the CNT dispersion, CNT and 2 wt% sodium cholate were first added to the dispersion medium and dispersed using an ultrasonic homogenizer [24]. This solution was placed in a spray can and used as a spray. After creating the SWCNT electrode film on the elastomer, several locations were randomly selected and the thickness was measured with a Keyence double scan high-precision laser measuring instrument (LT-9500 & LT-9010M), all of which were 50 μm. In addition, in order to confirm the degree of dispersion of the SWCNTs, SWCNTs before and after dispersion were confirmed by SEM.

The membrane size used was 20 mm (diameter) for the pressure sensor and 10 mm × 20 mm for the stretch sensor. Both film thicknesses were 200 μm.

3.4. Measuring capability of DEPS

The change in capacitance caused by the deformation of the DEPS using the method above was measured with an NF LCR METER (ZM2372).

3.4.1. Measuring capability of DEPS

Figure 2 shows the prototype DEPS using HNBR ver.6. This DEPS has a diameter of 20 mm and uses the Ver.6 with a

thickness of 200 μm as the main material. Electrodes were created using the CNT spray introduced above. The Ver.6 is extremely soft, so, by attaching this to a sheet (supporting material) made of H05-100J manufactured by Exeal Co., Ltd., a structure can be deformed even with a small load. The H05-100J urethane material used here has a hardness of Asker C0/7, which is relatively soft.

Figure 2
The prototype of a DEPS using HNBR: (a) Photograph of the DEPS; (b) A cross-section of the CPS

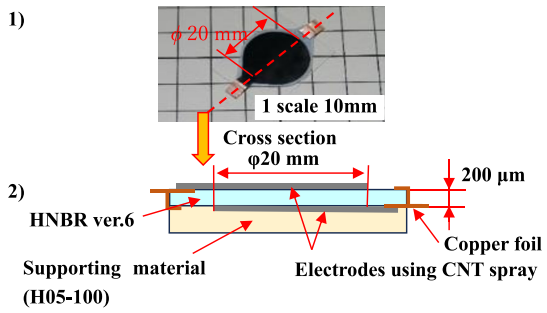

To confirm that the SWCNTs were uniformly sprayed onto the elastomer surface, four points on the surface of the DE sample were arbitrarily selected and observed using SEM.

3.4.2. Overview of the experimental system

Figure 3 is the test bench for the DEPS. A micrometer was attached to the *XYZ* axis precision stage, and a load was applied from above the DEPS to deform it and measure it. The DEPS used in the experiment was attached to the top of the load cell installed on the *XYZ* axis precision stage. Two load cells with maximum measurement loads of 2 and 10 kg were used for measurement due to the measurement range. The analog signal output from the load cell was input to the microcomputer (ATmega328) via a dedicated AD conversion IC (HX711). After that, calibration processing was performed by the microcomputer, and the measured with electronic venire calipers were displayed on the LCD. For the load measurement accuracy, it was confirmed that the error was 5% or less using a weight whose mass had been measured in advance.

Figure 3
Overview of the test bench used for the DEPS experiment

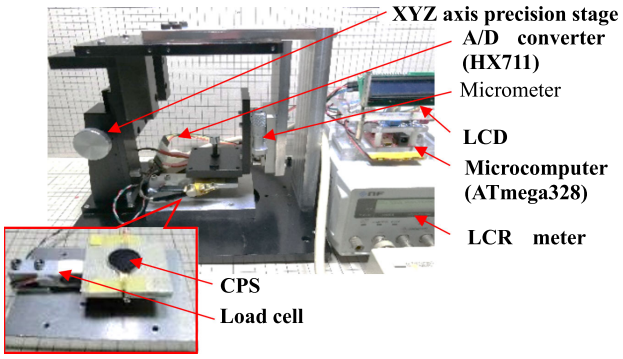

CPS installed on the test bench

3.5. Measurement of the stretchability of DESS

Outlines of the DESS used in the experiment and the experiment system are described in next sections:

3.5.1. Overview of the DESS used in the experiment

Figure 4 shows the prototype of the DESS using HNBR ver.6. The basic configuration is the same as the *p* described in Section 3.4. However, in consideration of attaching it to a robot hand, the shape is a rectangle of 10 mm in length and 20 mm in width, and no support material is used.

Figure 4
The prototype DESS

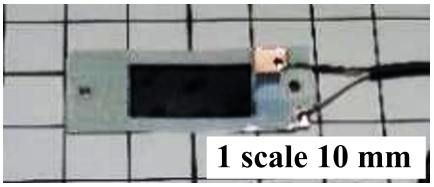

3.5.2. Overview of the DESS system for the experiment and experimental method

The test bench for the DESS has a structure in which the movable part moves between the linear slides attached to the fixed part. A DESS can be stretched by fixing both ends to a fixed part and a movable part and then rotating the ball screw. The stretched length was measured with digital calipers attached to the fixed and movable parts, and the capacitance was measured using an LCR meter (ZM2372) manufactured by NF Corporation. Figure 5 shows the prototype of the DESS using HNBR ver.6. Figure 10 shows the test bench for the DESS.

Figure 5
The test bench for the DESS

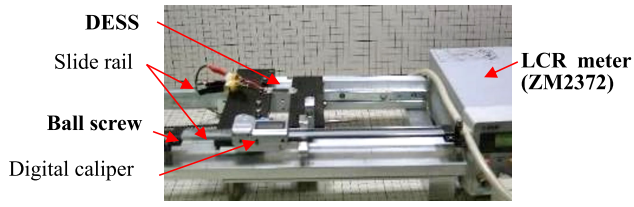

The method for measuring capacitance is shown as follows. The unstretched length of the DESS was set to 0 mm (see Figure 19(a)). From that point, it was stretched to 80 mm (Figure 19(b)) and the capacitance was measured.

3.6. Measurement of DES response speed

The response speed of the DEPS was verified by measuring the time from when the capacitance started to change when a sudden load was applied to the DEPS until the time it stabilized. The DEPS used in the experiment has the same specifications as in Section 3.4. A weight of 10 gf was dropped from a height of 10 mm onto the DEPS mounted on the aluminum plate, and the change in the detected capacitance was converted into a voltage by the detection

circuit. In the case of DESS, the response speed of the DESS was verified by measuring the time from when the DESS was stretched (or pressured) on the test bench to when the capacitance started to change. The DESS used in the experiment has the same specifications as in Section 3.5. The DESS was stretched by a stepper motor attached to the test bench. In addition, the extension start timing was detected by a 3-axis acceleration sensor (ADXL-345 manufactured by ANALOG DEVICES Inc.) attached to the test bench.

The change in DESS is converted to voltage by the detection circuit and measured along with the start of the decompression starts via a 16-bit A/D conversion IC (ADS1115) made by TEXAS INSTRUMENTS and a microcomputer (ATmega328P) made by Atmel. Figure 6 shows how the DES response speed is measured.

Figure 6
Measuring the response speed of a DES

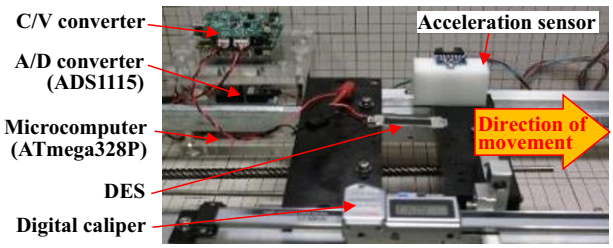

As with the DESS, changes in DEPS capacitance were converted to voltage by a detection circuit and measured via a 16-bit A/D conversion IC (ADS1115) made by Texas Instruments and a microcomputer (ATmega328P) made by Atmel.

3.7. Measurement of robot finger movement and finger pressure, and an experiment to transmit the sensation of the robot finger touching an object to a human finger

First, the motion of the robot's finger was sensed using a DESS, and the force (pressure) when the fingertip touched the object was measured. Figure 7 shows the DESSs and DEPSs attached to the robot hand.

Five DEPSs were used and attached to the tip of each finger. The shape of the pressure sensor was a circle with a diameter of 20 mm. The stretch sensor was a rectangle of 20 mm in length and 10 mm in width. Five stretch sensors were attached to the base of each finger. Each DEPT/DESS detection circuit consists of a C/V converter and a high-gain amplifier. By arranging it on the back of the hand, the analog signal wiring can be shortened, preventing malfunctions due to noise, making it possible to detect minute signal changes (see Figure 12).

Figure 7
The DESSs and DEPSs attached to the robot hand

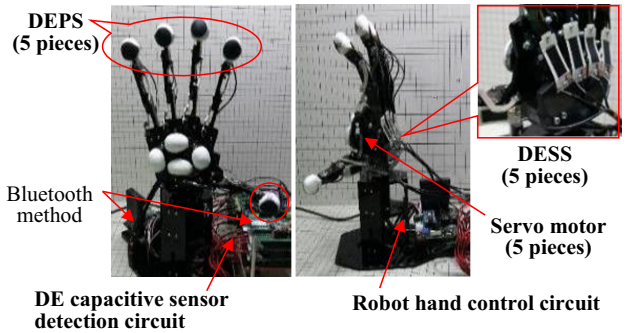

Five micro servo motors (product model number: MG90S) with a maximum torque of 2.2 kgf · cm and a weight of 13 gf were used to drive the fingers. Figure 8 shows a block diagram of the drive system and sensing circuit of the robot hand.

Figure 8
Block diagram of the drive system and sensing circuit of the robot hand

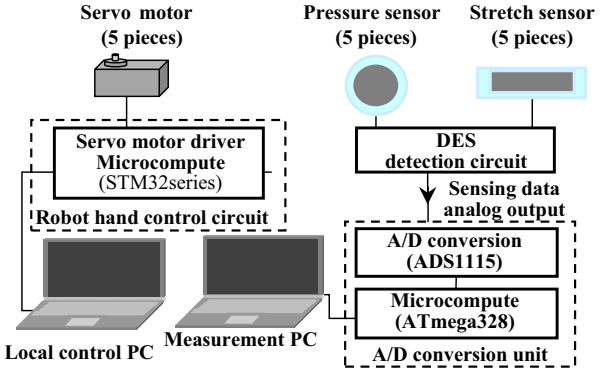

A microcomputer (STM32 series) manufactured by STMicroelectronics was used to drive the robot hand. Also, by connecting the microcomputer and the local control PC with a USB cable, it can be moved like a human hand. A pressure sensor and a stretch sensor are attached to each finger. The signals detected by these sensors were converted to analog signals by the detection unit, converted to digital signals by the A/D conversion unit, and then recorded by the measurement PC. The A/D conversion unit used for the measurement consists of a 16-bit A/D conversion IC (ADS1115) manufactured by TEXAS INSTRUMENTS and a microcomputer (ATmega328P) manufactured by Atmel (see Figure 9).

Figure 9
State of driving experiment of robot hand

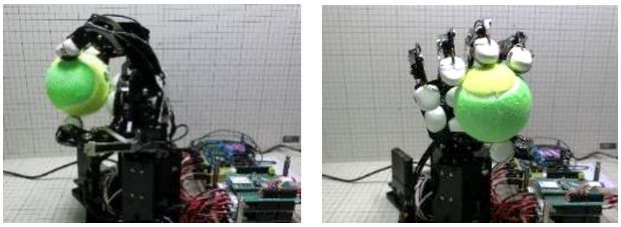

Figure 9 shows a driving experiment of a robot hand equipped with the DEPS and the DESSs. Using this system, the detection status of the DEPS and DESS was confirmed by holding the ball with the thumb and index finger.

By bending the index finger of the robot hand, it was confirmed that the detection signal of the stretch sensor increases. Also, it was confirmed that the pressure sensor responds when the tip of the index finger touches the ball. In addition, an experiment was also conducted to transfer human finger movements to robot fingers. Furthermore, an experiment was conducted in which a small diaphragm-type vibration DEA (active part diameter: 6 mm) [40] was applied to a human finger to feed back the sensation of the robot finger touching an object to the human finger. Figure 10 shows how a small diaphragm-type vibration DEA is attached to a human hand. Figure 10(a) is a small diaphragm-type vibrating DEA. The donut-shaped black parts are the electrodes, which are placed in front and back with the elastomer sandwiched between them. Figure 10(b) shows a small diaphragm-type vibration DEA unit mounted in a control sensor glove. The brown part is insulating tape made of polyimide. Fingers and the DEA are held in the glove by acrylic DEA folders.

Figure 10
Attaching a small diaphragm-type vibration DEA to the fingertip: (a) a small diaphragm-type vibration DEA; (b) the DEA attached to a human finger

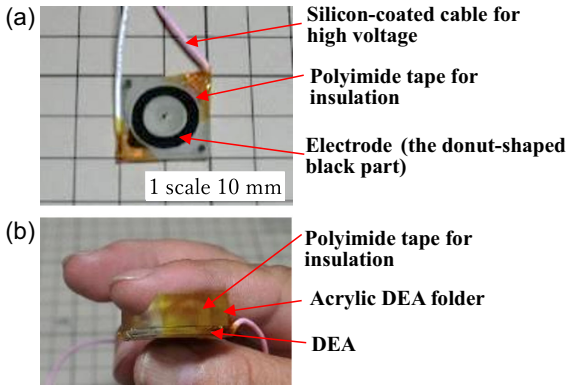

The DEA had an outer diameter of 6 mm, and the elastomer used was 3M/4905. Electrodes were made by spraying SWCNTs [28]. As mentioned above in how to make a DEPS, the reason why HNBR ver.6 was not used for this vibrator DE is that the ver.6 was too soft for the DE.

Next, Figure 11 shows a block diagram of the driving system and sensing circuit of the robot hand, the sensor glove, and the small diaphragm DEA-driving system.

The drive system and sensing circuit of the robot hand are almost the same as those shown in Figure 8 above, but the following points have been changed in order to connect the operating sensor glove and the small diaphragm DEA drive system.

The first change is that in Figure 11, the servo motor drive signal was supplied from the local control PC, but in this system, the servo motor drive signal is supplied from the operation sensor glove via the wireless module. This makes it possible to remotely control the robot hand from several meters away. The second change is that the signal detected by the pressure sensor is used as the drive signal for the small diaphragm DEA. In this system, the analog signal detected by the pressure sensor is converted into a digital signal by the microcomputer (ATmega328) installed in the A/D converter unit and supplied to the drive system of the small diaphragm DEA via the wireless module. Next, an overview of the operation of the

Figure 11
Block diagram of the drive system and sensing circuit of the robot hand, the operating sensor glove, and the small diaphragm-type DEA drive system

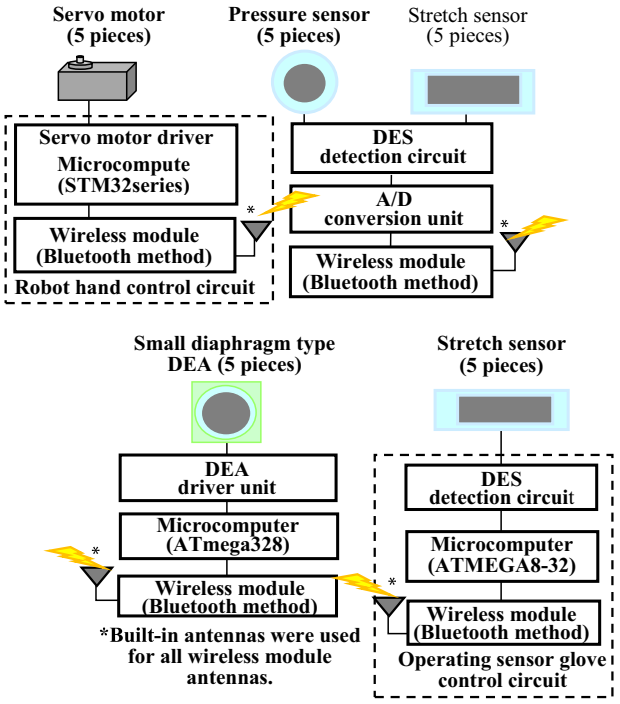

operation sensor glove and the drive system of the small diaphragm DEA will be described. A finger movement is detected as a change in capacitance by a stretch sensor attached to the operation sensor glove. The detected change in the DES capacitance is converted to an analog signal by the detection circuit and supplied to an Atmel microcomputer (ATmega8-32). The drive signal for the small diaphragm DEA is generated by a microcomputer (ATmega328) based on the pressure signal supplied from the robot hand, adjusted to an appropriate voltage by the DEA driver, and then supplied to the small diaphragm DEA. Figure 12 shows how the prototype robot hand is controlled by the operation sensor glove.

Figure 12
Prototype robot hand and operation sensor glove

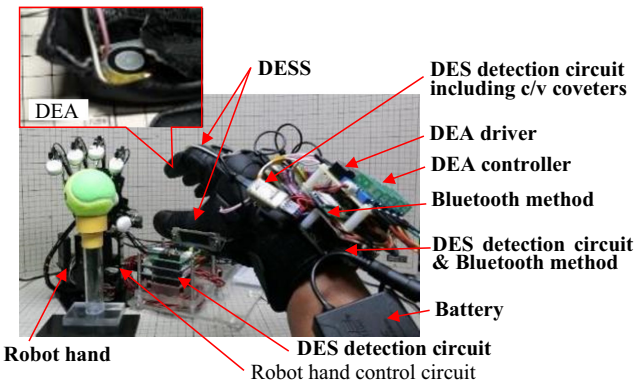

4. Results

The results of the experiments described in the experimental methods above are shown below.

4.1. Adjustment of HNBR additives and reduction of dangling bonds

Table 2 shows the results of the adjustment of HNBR additives and reduction of dangling bonds.

In the previous experiment, ver.3 was used, and the measurable pressure ranged from 4 to 120 kgf [24]. However, this time, this experiment was conducted using the softer ver.6 in order to be able to measure lower pressures, as shown in Table 2.

4.2. Results of the tensile tests

Figure 13 shows the results of a tensile test using HNBR with adjusted additives and reduced dangling bonds.

Compared to the original HNBR (before the improvement), when looking at Ver.3 and Ver.6, it can be seen that the elongation has increased sufficiently in Ver.6.

Figure 13
HNBR tensile test results

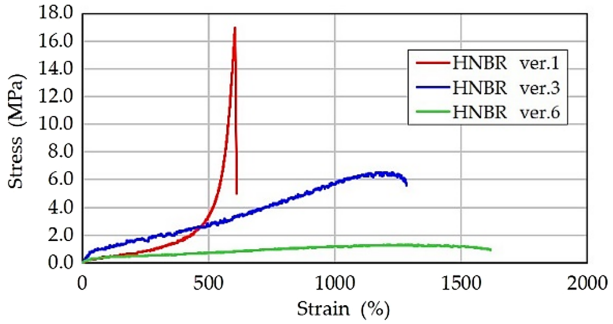

4.3. Confirmation of the degree of dispersion of SWCNTs and confirmation of the electrode surface with SWCNTs sprayed on elastomer

The SWCNTs were well dispersed to create a SWCNT spray. Figure 14(a) shows SEM photographs before and after dispersion. As shown in Figure 14(a), it can be seen that they are sufficiently dispersed. In addition, electrodes were created using CNT spray, and to confirm this, the electrode surfaces were observed using SEM. As a result, it can be seen that the CNTs were sprayed uniformly in Figure 14(b). The thickness was also measured at three locations, and all were confirmed to be 50 μm.

4.4. Measurement results of the pressure DES

For the measurement, the length of the micrometer attached to the *XYZ* axis precision stage was adjusted to increase the load applied to the CPS, and the capacitance at each load was measured. As shown in Section 3.4.2 above, since the measurement range of the load cell used this time is narrower than the measurement range of the CPS, the measurement range was divided into two ranges, 1 to 2 kgf and 2 to 20 kgf. The measurement results of the two ranges are summarized in Figure 15.

Figure 14
SWCNTs before and after dispersion and electrode surface by spraying SWCNTs: (a) SWCNTs before and after dispersion (magnification: X10,000), (a)-1 SWCNT before dispersion, (a)-2 SWCNTs after dispersion; (b) Electrode surface by spraying SWCNTs, (b)-1 Magnification: X1,500, (b)-2 Magnification: X5,000

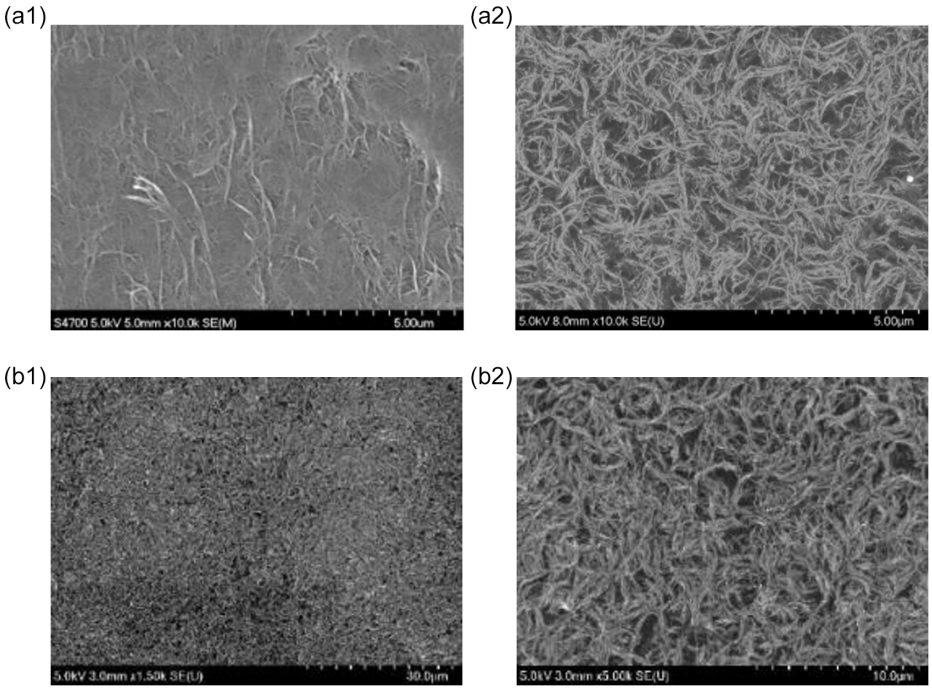

Figure 15
The capacitance when a load of 1 gf to 20 kgf is applied

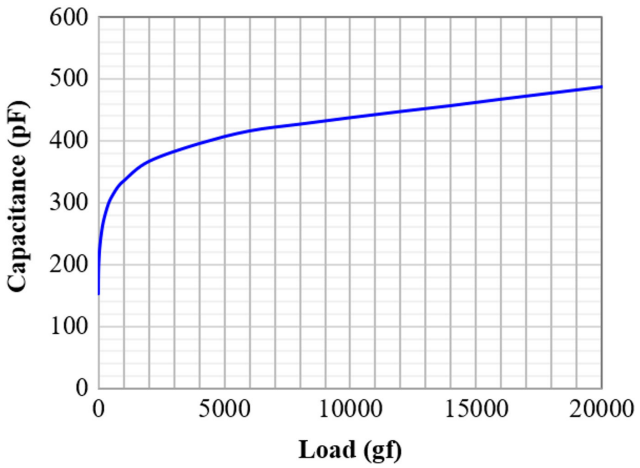

4.5. Measurements of the DES' response speeds

Figure 16 shows the change in the measured DESS capacitance. A is the point where the DESS displacement begins, and B is the point where the capacitance begins to change. The time from point A to point B was 50 ms, and it was confirmed that sufficient driving speed was obtained for use in a robot hand. Thus, the response speed of the DESS was 50 ms.

Figure 16
Changes in measured capacitance

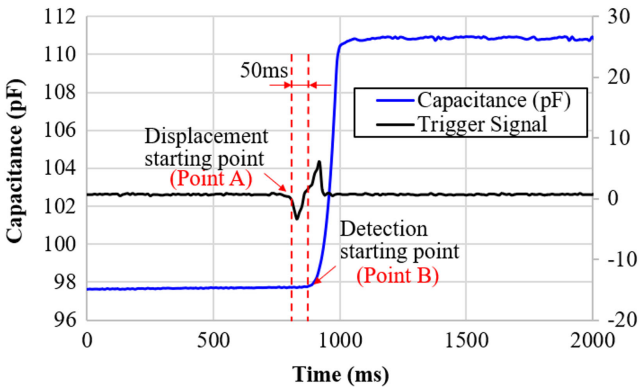

In the case of DEPS, according to the measurement method in Section 3.6 above, the speed of the pressure was measured and it was 50 ms, that is also fast enough.

4.6. DES stretching ability measurement results

Figure 17 shows the changes in capacitance when the DESS is stretched. As shown in Section3.5.2, as the method for measuring capacitance, the unstretched length of the DESS was set to 0 mm (see Figure 18(a)). From that point, it was stretched to 80 mm (Figure 18(b)) and the capacitance was measured. Since the length of the sensor part of the DESS is 20 mm (see Figure 4), it was confirmed that the sensor can be stretched by 400% (see Figure 18(b)). It can be seen that even with a slight elongation of about 10%, the capacitance changes, and even with an elongation of more than 400%, the capacitance changes almost linearly. Figure 18 shows a photograph of the DESS over 400%. Moreover, even after being stretched over 400%, it still remains conductive and it can be seen that sensing is possible.

Changes in capacitance with an LCR meter while stretching were measured. The elongation was measured using a digital caliper, and the lengths were compared. In both cases, an electric current was applied to check the conductivity, and the LED was turned on.

Figure 17
A graph showing changes in capacitance when the DESS is stretched

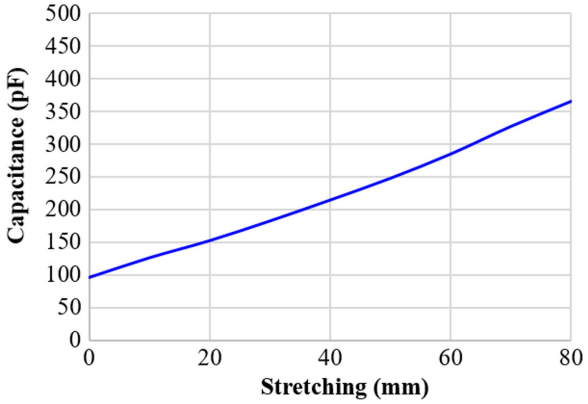

Figure 18
Photographs of the DESS stretched over 400%: (a) before stretching; (b) after stretching

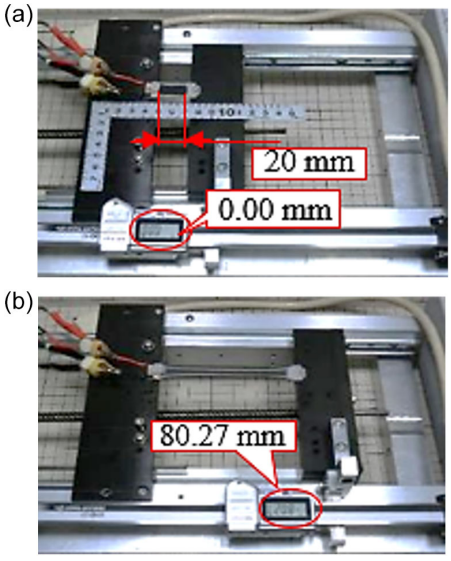

4.7. System of the pressure felt by a robot's finger and the transmission of the robot's finger sensation touching an object to a human finger

Using a robot hand drive system equipped with a DEPS and a DESS, the detection status of the pressure sensor and stretch sensor

was confirmed by holding the ball with the thumb and forefinger. Figure 19 shows transitions of analog signals of fingertip pressure and finger displacement detected by the pressure sensor and the stretch sensor at this time.

Figure 19
The fingertip pressure and finger displacement detected by the pressure sensor and stretch sensor attached to the index finger of the robot hand: (a) Movement to hold the ball with the thumb and index finger; (b) Transitions of the analog signals of fingertip pressure and finger displacement detected by the pressure sensor and the stretch sensor

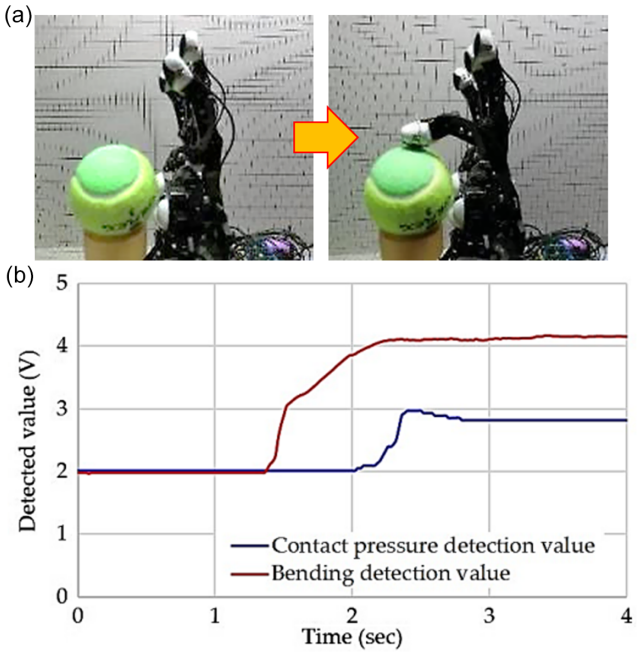

Figure 20 shows the robot hand being operated by the sensor glove worn on the hand. It was confirmed that the same movements as the hand can be reproduced with the robot hand.

5. Discussion

As mentioned above, using 3M acrylic film (4905), the pressures that can be measured up to now range from about 5 to about 120 kgf, and pressures lower than about 5 kgf could not be measured [24]. However, this time it became possible to measure from 1gf to 20 kgf (see Figure 16). A major factor behind this is that the yield point stress values of 3M acrylic film (4905) and HNBR ver.6 are about half or less (see Figures 13 and 21). In other words, even if a little pressure is applied, the film can be deformed, and the slight change in capacitance can be measured.

This HNBR DEPS can measure any pressure anywhere within the measuring range from 1 gf to 20 kgf (see Figure 15). The reason for this is that, as mentioned above, it has been made softer in HNBRF Ver.6. However, since this Ver.6 is very soft, the H05-100UJ urethane material is used as a support material under this sensor in order to increase its strength (see Figure 2). Because this material was stiffer than urethane, the applied pressure could be distributed better on the sensor, helping the DEPS deform through its thickness even with small forces. Moreover, the reason why the DEPT has a circular shape is to uniformly receive the pressure from above. As explained in Section 3.4.2, incidentally, in order to increase the accuracy of the applied force, load cells were used to apply a load from the top of the CPS to deform it and measure it. Electrodes are also important in DEPTs and DESSs [24]. The thickness of the electrode used this time was 50 μm. This is because very thin electrodes deform better. However, the thin electrode requires the SWCNTs to be sufficiently dispersed, and as shown in Figure 14(a), they were sufficiently dispersed in this experiment. It is also important that the electrodes, along with the elastomer, remain conductive even when deformed. Using a hand-held SWCNT sprayer, the electrodes can be applied very carefully, allowing the creation of very thin electrodes while remaining conductive. [28]. As shown in Figure 14(b), the SWCNT has a tubular elongated shape, and even if the electrode is stretched, the elongated shape can contact each other at somewhere and can maintain conductivity [25]. Incidentally, the SWCNTs have an average diameter of 3 to 5 nm and an average length of 80 to 100 μm. Moreover, another point is that it depends on the circuit design (see Section 3.4). A higher amplification circuit consisting of a C/V converter and a high-gain amplifier can also be used to measure smaller changes, thus increasing the measurement range (see Figure 12). In other words, the pressure measurement range of the DEPS changes depending on the hardness of the material used, the shape of the sensor, the tuning of the detection circuit, etc., so it is important to select those specifications according to the purpose [24]. From those results, it is possible to improve the performance. In this experiment, the response speed of this DEPS was 50 ms (see Figure 16). This response speed, like pressure measurement, also depends on the hardness of the film and the circuit. Additionally, because the performance of the servo motor was not fully optimized, the

Figure 20
Manipulation of the robotic hand using the manipulator sensor glove: (a) grasping using all fingers; (b) opening index and middle fingers; (c) opening all fingers

contact pressure detection value and bending detection value could be a little jagged (see Figure 19).

Table 3 shows the response speed of the pressure sensor for different elastomer types and electrode types [24]. As shown in Figure 21, it can be seen that the silicon material is harder than other films, and as seen in Table 2, it has a fast response speed as a sensor. However, due to its small elongation, its application is considered to be limited. In other words, materials with low dynamic viscoelasticity, such as silicon, are not suitable DEA/ sensor materials [24]. On the other hand, acrylic and HNBR are softer and more elastic than other films, making them suitable materials for sensors. The response speed is also sufficient for practical use, and it seems to be optimal as a sensor that is used in close contact with a person's finger.

Table 2
Adjusting HNBR additives and reducing dangling bonds

	Cross-linking agent (when rubber is 100)	Cross-linking agent name	Crosslinker (molecular weight)	Double bond amount (%)
HNBR original film	8	1,3 1,4-bis (t-butyl alcohol isopropyl alcohol) Benzene	338.5	10
HNBR film ver.1	8	Same as above	338.5	5
HNBR film ver.3	2	Same as above	338.5	1
HNBR film ver.6	1	Same as above	338.5	1

Table 3
Difference in response speed when changing the type of elastomer and electrode

	Response speed (ms)		
	Carbon grease	Carbon black	SWCNT
Silicone material (ELASTOSIL FILM 2030 250)	69	66	59
HNBR Ver.3	80	78	68
Acrylic material made in the United States (3M/4905)	93	86	73
The film that corrected the distortion of the 3M/4905 acrylic	94	88	74

Note: Each of the above measurement data was confirmed in the load cell. The unit of speed is milliseconds

It was found that the capacitance of this DESS changes even when it is stretched by only about 10%, and the capacitance changes almost linearly even after even being stretched by more than 400% at log scale (see Figures 17 and 18). Also, the speed of

Figure 21
The results of the SS curves of the silicon (ELASTOSIL FILM 2030 250: shown in blue), the acrylic material made in the United States (3M/4905: shown in black), and the HNBR (ver.3: shown in orange and ver.6: shown in pink)

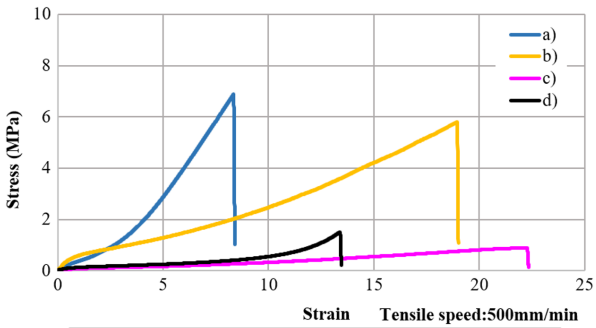

a) Silicone material (ELASTOSIL FILM 2030 250)
b) HNBR Ver.3
c) HNBR Ver.6
d) Acrylic material made in the United States (3M / 4905)

DESS was 50 ms. In this experiment, the DESS was attached to a tightly fitted glove. As a result, the sensor responded to the bending motion of the glove (fingers), and the motion could be transmitted to the robot quickly in a synchronized state. In other words, it seems that this sensor speed was sufficient. A DESS, like a DEPS, also depends on the stiffness of the membrane. In the case of the circuit, as mentioned again, using a higher amplification circuit allows smaller changes to be measured, increasing the measurement range. Thus, the elongation of this sensor depends on hardness, as it does with pressure.

It was also confirmed that the feeling of the robot fingertip touching the ball was obtained from the small diaphragm DEA attached to the operation sensor glove for a human operator (see Figures 19 and 20). In this system, the DEPS attached to the fingertip of the robot hand changes its capacitance according to the pressure of the fingertip contacting an object (see Figure 19). The change in capacitance is converted into a voltage signal by the DE capacitive detection circuit, converted into a digital signal by the A/ D conversion unit, and supplied to the microcomputer. The digital signal supplied to the operation sensor glove via the wireless module is supplied to the DEA-driving microcomputer and converted to a voltage signal to drive the small diaphragm-type DEA. This voltage signal is converted to a voltage (high voltage) for driving the DEA by the DEA driver unit and supplied to the small diaphragm-type DEA. On the other hand, the operation sensor glove has a DESS attached in order to each finger to sense the movement of each finger. The DESS changes its capacitance according to how the finger bends. This change in capacitance is converted into a voltage signal by the DE capacitive sensor detection circuit and supplied to the analog input of the microcomputer. This voltage signal is converted into a digital signal in the microcomputer, supplied to the robot hand via the wireless module, and used as a signal to drive the servo motor. In this prototype system, four microcomputers and four wireless modules are used to construct the system, but by reviewing the circuit, it is thought that the number of these used can be reduced to about half. Also, since the wireless module used this time uses the Bluetooth method, the operation range was several meters, but by changing the wireless module to the Wi-Fi method, the operation range can

be extended to several tens of meters. With these changes, it has become possible to move the robot's finger in real time in accordance with the movement of a human.

Furthermore, if the Internet is available, it can be operated from anywhere in the world. The use of 5G and 6G technology, which has been expanding in its use, will enable low-latency operation, so it can be applied to fields such as telemedicine that require precise operation. HNBR Ver.6 at this time is not suitable for DEAs because the adjustment method of the amount of cross-linking agent and the adjustment of dangling bonds were altered considerably, so the hardness was considerably reduced, so the strength of the film was low. Therefore, 3M/4905 was used in this experiment.

Moreover, if this DESS has the capability to be used as a three-dimensional position sensor for the arms and legs of robots and the like. To explain step by step, first a stretch sensor would be attached to the upper side of the arm of the robot. When the arm is moved upward, the upper sensor is contracted, and the lower sensor is extended, so that it is possible to two-dimensionally determine at what angle the arm is bent. Furthermore, if another pair of sensors are arranged on the side of the arm, sensing diagonal movement is also possible. That is, the three-dimensional position can be easily determined from the difference in dielectric constant between the top and bottom and the difference in dielectric constant between the sides. Therefore, it is beneficial to prepare such a calculation table in the microchip.

It is expected that robots will work together with humans in the very near future, and it is necessary to match the movements of humans, so humanoid robots are desired. However, as the frequency of contact with humans increases, it is essential for robots to be safe for humans. For example, when a robot's hand touches a person, an excellent sensor can instantly determine that it is a person and stop the robot's movement or sufficiently reduce its output.

With this human-robotic interaction system shown above, a physician can possibly use a virtual system to palpate a patient when the patient is at a remote location [28]. In addition, in the assembly of a machine, when performing a detailed and sensitive assembly, it might be possible for a robot to do such work alone someday, although it still requires a skilled human at present. Using this system and AI, a robot could be taught the movements for its hands and fingers. As another example, it will become possible to feel the sensations of shaking a hand or hugging someone virtually. As a step to realize the above-mentioned goals, the points obtained in this experiment might be a guideline for making an AI robot that could move and make decisions like humans in the future.

In 2012, the authors developed a system for the rehabilitation of patients who could not move their fingers due to conditions such as cerebral infarction by setting a DESS capable of measuring the stretch of the patients' fingers and measuring how much they can move their fingers [24]. However, the CSS at that time was not able to obtain sufficient elongation, which made it difficult to measure. However, with the new system, sufficient elongation can be obtained, so it is thought that the measurement can be performed accurately. Also, it is necessary to move the patient's fingers with external force during rehabilitation, but until now, the DEA has not been able to handle this sufficiently due to its low output. However, in 2021, the DEA device developed by Chiba et al. was successfully drove an 8kgf weight in 88ms with a DE of 0.15g [28, 40]. If this DEA device could be used, it would be possible to realize such a rehabilitation system without any problems.

As an electrode material, compared to multi-walled CNTs (MWCNTs) and carbon black, SWCNTs are more conductive, allowing for thinner electrodes and greater stretchability [24]. In this experiment, as mentioned above, the SWCNTs were sufficiently dispersed, so even if the SWCNTs were packed in the spray, they could be sprayed without clogging (see Figure 14(a) and (b)) [40].

6. Conclusion

In this experiment, a DEPS able to measure low pressure, a DESS capable of being greatly deformed, and a small diaphragm vibrating DEA were created. The following results were obtained by combining them.

- A DEPS was created using a very thin hydrogenated nitrile rubber (HNBR) film (0.2 mm) with improved hardness and elongation. It enabled measurement at any pressure between 1 gf and 20 kgf.
- In addition, a DESS with an elongation of 400% or more was developed using the same HNBR.
- Both a DESS and a DEPS were attached to the finger of the robot, and the movement of the finger was sensed and the force (pressure) when the finger touched the object was also able to be detected.
- In order to drive the robot's fingers as the human operator wished, a system was created in which the movements of the human fingers are transmitted to the robot's fingers by attaching the stretch sensors to the finger parts of the gloves made for humans and also to the robot's fingers. As a result, it became possible to move the robot's fingers following the human's movement.
- A vibrator using a small diaphragm DEA (the diameter of 6 mm) was attached to the human fingertip so that when the robot finger touched the object, the sensation of the robot's fingertip was able to be transmitted to the human finger. As the result, it is now possible to add sensations artificially.

The results obtained from this experiment will hopefully serve as data to further promote the development of robots that can be operated remotely by humans to perfectly reproduce the movements desired by humans, as well as the development of systems that can feed back the sensations of contact from robots. In addition, there is a strong demand for the realization of AI robots that can make more human-like movements and decisions using DEAs as the artificial muscles [28, 40].

Funding Support

We would like to thank Mr. M. Uejima, Mr. H. Uchida, and Mr. M. Takeshita of ZEON Corporation for providing SWCNT (ZEONANO®-SG101) and HNBR free of charge for carrying out our experiment.

Ethical Statement

This study does not contain any studies with human or animal subjects performed by any of the authors.

Conflicts of Interest

The authors declare that they have no conflicts of interest to this work.

Data Availability Statement

Data sharing is not applicable to this article as no new data were created or analyzed in this study.

References

[1] Sarutani, T., Takahashi, K., Aga, T., & Yamagata, T. (1991). Small integrated pressure sensor. *The Institute of Electronics, Information and Communication Engineering*, *J74-C2*(5), 333–339.

[2] Shirakawa, H. (2019). Discovery of conductive polymers and conductive mechanism. *Journal of Chemistry and Education*, *67*(2), 82–85. https://doi.org/10.20665/kakyoshi.67.2_82

[3] Harada, Y., Suehara, T., Ueno, T., & Higuchi, T. (2006). Development of an Actuator using Thermal Deformation. In *Proceedings of the Spring Meeting of the Japan Society for Precision Engineering*, 803–804.

[4] Ichinose, S. (1991). Current status and future of new materials for sensors. *The Robotics Society of Japan*, *9*(7), 883–887.

[5] Zhang, L., Gao, M., Wang, R., Deng, Z., & Gui, L. (2019). Stretchable pressure sensor with leakage-free liquid-metal electrodes. *Sensors*, *19*(6). https://doi.org/10.3390/s19061316

[6] Ma, Z., Li, S., Wang, H., Cheng, W., Li, Y., Pan, L., & Shi, Y. (2019). Advanced electronic skin devices for healthcare applications. *Journal of Materials Chemistry B*, *7*(2), 173–197. http://doi.org/10.1039/C8TB02862A.

[7] Su, R., Park, S., Li, Z., & McAlpine, M. (2019). 3D printed electronic materials and devices. In S. M. Walsh & M. S. Strano (Eds.), *Robotic systems and autonomous platforms, advances in materials and manufacturing* (pp. 547–557). Elsevier.

[8] Al Moubayed, S., Beskow, J., Skantze, G., & Granström, B. (2012). Furhat: a back-projected human-like robot head for multiparty human-machine interaction. In A. Esposito, A. M. Esposito, A. Vinciarelli, R. Hoffmann, & V. C. Müller (Eds.), *Cognitive behavioural systems* (pp. 114–130). Springer Berlin Heidelberg.

[9] Ponraj, G., Kirthika, S. K., Thakor, N. V., Yeow, C. H., Kukreja, S. L., & Ren, H. (2017). Development of flexible fabric based tactile sensor for closed loop control of soft robotic actuator. In *13th IEEE Conference on Automation Science and Engineering*, 1451–1456. https://doi.org/10.1109/COASE.2017.8256308

[10] Au, A. K., Bhattacharjee, N., Horowitz, L. F., Chang, T. C., & Folch, A. (2015). 3D-printed microfluidic automation. *Lab on a Chip*, *15*(8), 1934–1941. https://pubs.rsc.org/en/contentarticlelanding/2015/lc/c5lc00126a/unauth

[11] Takenaga, S., Schneider, B., Erbay, E., Biselli, M., Schnitzler, T., Schöning, M. J., & Wagner, T. (2015). Fabrication of biocompatible lab-on-chip devices for biomedical applications by means of a 3D-printing process. *Physica Status Solidi (a)*, *212*(6), 1347–1352. https://doi.org/10.1002/pssa.201532053.

[12] Kumar, A. (2018). Methods and materials for smart manufacturing: Additive manufacturing, internet of things, flexible sensors and soft robotics. *Manufacturing Letters*, *15*, 122–125. https://doi.org/10.1016/j.mfglet.2017.12.014

[13] Kim, J., Alspach, A., & Yamane, K. (2015). 3D printed soft skin for safe human-robot interaction. In *IEEE/RSJ International Conference on Intelligent Robots and Systems*, 2419–2425. https://doi.org/10.1109/IROS.2015.7353705

[14] Agarwala, S., Goh, G. L., Yap, Y. L., Goh, G. D., Yu, H., Yeong, W. Y., & Tran, T. (2017). Development of bendable strain sensor with embedded microchannels using 3D printing. *Sensors and Actuators A: Physical*, *263*, 593–599. https://doi.org/10.1016/j.sna.2017.07.025.

[15] Laszczak, P., Jiang, L., Bader, D. L., Moser, D., & Zahedi, S. (2015). Development and validation of a 3D-printed interfacial stress sensor for prosthetic applications. *Medical Engineering & Physics*, *37*(1), 132–137. https://doi.org/10.1016/j.medengphy.2014.10.002

[16] Kirthika, S. K., Ponraj, G., & Ren, H. (2017). Fabrication and comparative study on sensing characteristics of soft textile-layered tactile sensors. *IEEE Sensors Letters*, *1*(3), 1–4. https://doi.org/10.1109/LSENS.2017.2708425

[17] Senthil Kumar, K., Ren, H., & Chan, Y. H. (2017). Soft tactile sensors for rehabilitation robotic hand with 3D printed folds. In *International Conference for Innovation in Biomedical Engineering and Life Sciences*, 55–60. https://doi.org/10.1007/978-981-10-7554-4_9

[18] Qiao, H., Zhang, Y., Huang, Z., Wang, Y., Li, D., & Zhou, H. (2018). 3D printing individualized triboelectric nanogenerator with macro-pattern. *Nano Energy*, *50*, 126–132. https://doi.org/10.1016/j.nanoen.2018.04.071

[19] Kumar, K. S., Chen, P. Y., & Ren, H. (2019). A review of printable flexible and stretchable tactile sensors. *Research*, *2019*, 32. https://doi.org/10.34133/2019/3018568

[20] Amjadi, M., Yoon, Y. J., & Park, I. (2015). Ultra-stretchable and skin-mountable strain sensors using carbon nanotubes–Ecoflex nanocomposites. *Nanotechnology*, *26*(37). https://doi.org/10.1088/0957-4484/26/37/375501

[21] Ahmed, F., Soomro, A. M., Ashraf, H., Rahim, A., Asif, A., Jawed, B., . . . , & Choi, K. H. (2022). Robust ultrasensitive stretchable sensor for wearable and high-end robotics applications. *Journal of Materials Science: Materials in Electronics*, *33*(35), 26447–26463. https://doi.org/10.1007/s10854-022-09324-0

[22] Jabbar, F., Soomro, A. M., Lee, J. W., Ali, M., Kim, Y. S., Lee, S. H., & Choi, K. H. (2020). Robust fluidic biocompatible strain sensor based on PEDOT: PSS/CNT composite for human-wearable and high-end robotic applications. *Sensors & Materials*, *32*, 12. https://doi.org/10.18494/SAM.2020.3085

[23] Khan, H., Soomro, A. M., Samad, A., Waqas, M., Ashraf, H., Khan, S. A., & Choi, K. H. (2022). Highly sensitive mechano-optical strain sensors based on 2D materials for human wearable monitoring and high-end robotic applications. *Journal of Materials Chemistry C*, *10*(3), 932–940. https://doi.org/10.1039/D1TC03519C

[24] Chiba, S., Waki, M. (2020). Dielectric elastomer sensor capable of measuring large deformation and pressure. In R. Vinjamuri (ed.), *Human-robot interaction-perspective and applications*. IntechOpen. https://www.intechopen.com/chapters/84850

[25] Chiba, S., & Waki, M. (2019). Application to dielectric elastomer materials, power assist products, artificial muscle drive system. In Technical Information Association (Ed.), *Next-generation polymer/polymer development, new application development and future prospects*. Technical Information Association.

[26] Ni, N., & Zhang, L. (2017). Dielectric elastomer sensors. In N. Cankaya (Ed.), *Elastomers* (pp. 231–253). IntechOpen. https://doi.org/10.5772/intechopen.68995.

[27] Rizzello, G. (2023). A review of cooperative actuator and sensor system based on dielectric elastomer transducers. *Actuators*, *12*(2), 46. https://doi.org/10.3390/act12020046

[28] Chiba, S. A., Waki, M., Takeshita, M., & Ohyama, K. (2023). Possibilities of artificial muscles using dielectric elastomers and their applications. *Advanced Materials Research*, *1176*, 99–117. https://doi.org/10.4028/p-jj7z4z

[29] Han, M., Lee, J., Kim, J. K., An, H. K., Kang, S. W., & Jung, D. (2020). Highly sensitive and flexible wearable pressure sensor with dielectric elastomer and carbon nanotube electrodes. *Sensors and Actuators A: Physical*, *305*. https://doi.org/10.1016/j.sna.2020.111941

[30] Willian, T. P., Fasolt, B., Motzki, P., Rizzello, G., & Seelecke, S. (2023). Effects of electrode materials and compositions on the resistance behavior of dielectric elastomer transducers, *Polymers*, *15*(2), 310. https://doi.org/10.3390/polym15020310

[31] Shigemune, H., Sugano, S., Nishitani, J., Yamauchi, M., Hosoya, N., Hashimoto, S., & Maeda, S. (2018). Dielectric elastomer actuators with carbon nanotube electrodes painted with a soft brush. *Actuators*, *7*(3), 51. https://doi.org/10.3390/act7030051

[32] Walker, C., Haller, M., Orbaugh, D., Freeman, S., Rosset, S., & Anderson, I. (2023). Polymer sensors for underwater robot proprioception. *Sensors and Actuators A: Physical*, *351*. https://doi.org/10.1016/j.sna.2023.114179.

[33] Vennemann, N., Kummerlöwe, C., Schneider, M., Bröker, D., Siebert, A., Teich, S., & Rosemann, T. (2023). Influence of unipolar electric fields on the behavior of dielectric elastomer actuators based on plasticized acrylonitrile-butadiene rubber (NBR). *Journal of Applied Polymer Science*, *140*(14). https://doi.org/10.1002/app.53694.

[34] Jung, K., Kim, K. J., & Choi, H. R. (2008). A self-sensing dielectric elastomer actuator. *Sensors and Actuators A: Physical*, *143*(2), 343–351. https://doi.org/10.1016/j.sna.2007.10.076

[35] Böse, H., & Fuß, E. (2014). Novel dielectric elastomer sensors for compression load detection. In *Electroactive Polymer Actuators and Devices*, *9056*, 232–244. https://doi.org/10.1117/12.2045133

[36] Böse, H., & Ehrlich, J. (2023). Dielectric elastomer sensors with advanced designs and their applications. *Actuators*, *12*(3), 115. https://doi.org/10.3390/act12030115.

[37] Seelecke, S., Neu, J., Croce, S., Hubertus, J., Schultes, G., & Rizzello, G. (2023). Dielectric elastomer cooperative microactuator systems-DECMAS. *Actuators*, *12*(4), 141. https://doi.org/10.3390/act12040141.

[38] Walker, C. R., & Anderson, I. A. (2017). Monitoring diver kinematics with dielectric elastomer sensors. In *Electroactive Polymer Actuators and Devices*, *10163*, 11–21. https://doi.org/10.1117/12.2260394

[39] Venkatraman, R. J., Kaaya, T., Tchipoque, H., Cluff, K., Asmatulu, R., Amick, R., & Chen, Z. (2022). Design, fabrication, and characterization of dielectric elastomer actuator enabled cuff compression device, In *Electroactive Polymer Actuators and Devices XXIV*, *12042*, 32–40. https://doi.org/10.1117/12.2613250

[40] Chiba, S., Waki, M., Takeshita, M., Yoshizawa, T., Yoshizawa, Y., & Yoshizawa, K. (2021). Application of dielectric elastomer to actuators, robots, power assist devices, etc. In Technical Information Institute Co. (Ed.), *Design of conductive materials, conductivity control and latest application development*. Technical Information Institute Co.

How to Cite: Chiba, S. & Waki, M. (2023). Excellent Miniature Thin Film Dielectric Elastomer Sensors for Robot Fingers Used in Human-Robot Interaction. *Archives of Advanced Engineering Science* https://doi.org/10.47852/bonviewAAES32021716